State of the art treatment of cirrus clouds in climate models

Ulrike Lohmann

Department of Physics and Atmospheric Science,
Dalhousie University, Halifax, N. S., Canada

Contributions from

Johannes Hendricks and Bernd Kärcher, (DLR, Oberpfaffenhofen)

Claudia Timmreck (MPI for Meteorology)

How do GCMs treat cirrus clouds?

- Historically GCMs predict only the condensed water content and use a temperature dependence to distinguish between the ice and liquid phase
- Lately, ice and water clouds are treated separately in most GCMs
- Wilson and Ballard (1999) were the first to allow supersaturation with respect to ice by explicitly solving the growth equation for a single ice particle
- Lohmann (2002) introduced a prognostic equation for the number of ice crystals and Lohmann and Kärcher (2002) got rid of the saturation adjustment scheme as well, which enables us to study homogeneous and heterogeneous freezing leading to cirrus cloud formation.

Outline of my Talk

- *Homogeneous freezing* of supercooled aerosols:
  - theory
  - parcel model results
  - climate model results
- *Heterogeneous freezing*
  - observations
  - parcel model results
  - climate model results
- *Conclusions*

Homogeneous freezing of supercooled aerosols

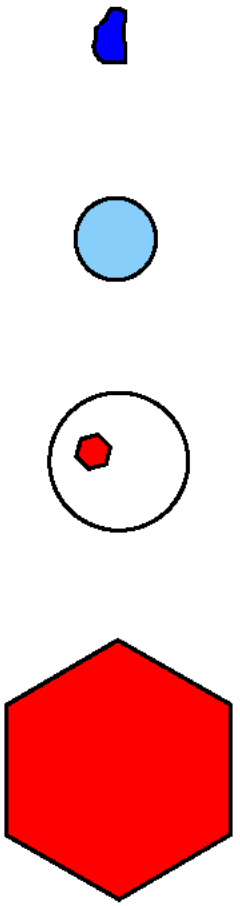

- freezing rates are well-established; field data support lab results
- important ice formation mechanism in the UT (and LS)
- role of heterogeneous processes unclear

First step in the development of a physically-based parameterization of cirrus formation.

Adiabatic parcel model *[Lin et al. 2002]*

- 79 size bins for ice crystals
- 56 size bins for aerosols

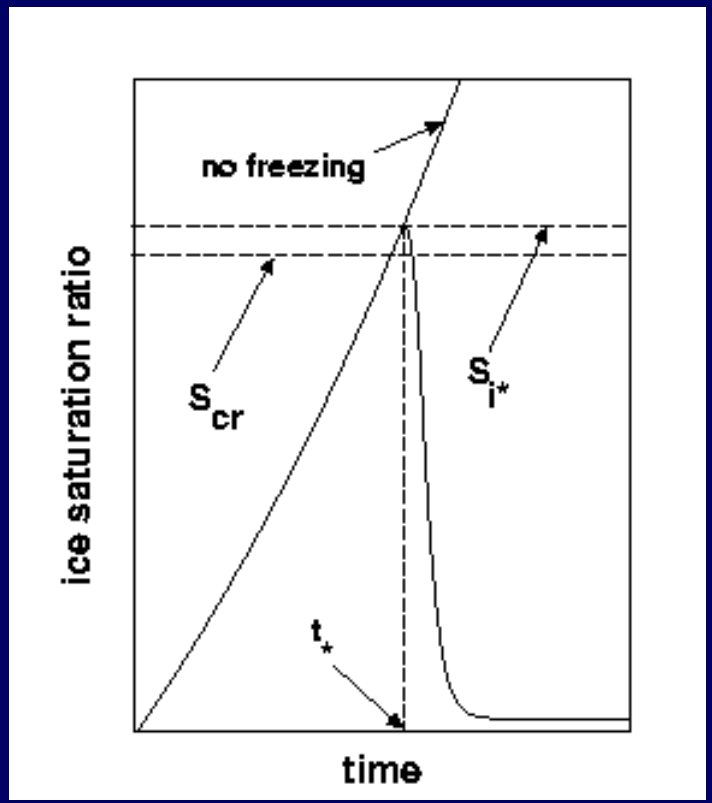

RH

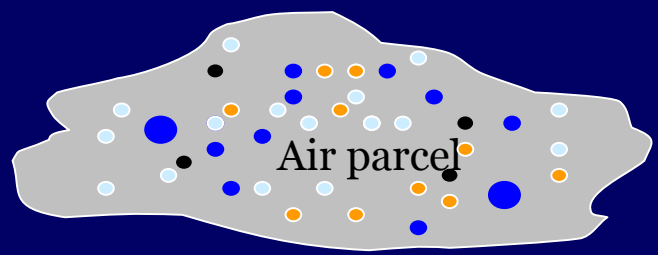

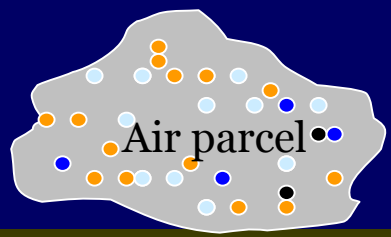

Governing equations

$$\frac{dS_i}{dt} = a_1 S_i w - \left(a_2 + a_3 S_i\right) R_i \qquad (1)$$

$$R_i = \frac{\rho_i}{m_w} \int_{-\infty}^{t} dt_0 \, \dot{n}_i(t_0) \, 4\pi r_i^2(t_0, t) \, \frac{dr_i}{dt}(t_0, t) \qquad (2)$$

$$\dot{n}_i = \int_{r_s}^{\infty} dr_0 \, \frac{4\pi}{3} r_0^3 J \frac{dn}{dr_0}, \quad n_i = \int_{r_s}^{\infty} dr_0 \, \frac{dn}{dr_0} \qquad (3)$$

$$\frac{dr_i}{dt} = \frac{b_1 \left(S_i - 1\right)}{1 + b_2 r_i} \qquad (4)$$

Freezing saturation ratios $S_{\mathrm{cr}}(T)$ according to:
Th. Koop et al., *Nature*, *406*, 611, 2000.

Solution strategy

- choose suitable ansatz for nucleation pulse
- evaluate (1) at the time where S_i reaches a peak

Two distinct timescales

$$\tau_f = \left[c \left| \frac{\partial \ln(J)}{\partial T} \right| \frac{dT}{dt} \right]^{-1} \qquad \tau_g = \left[\frac{b_1 (S_{\mathrm{cr}} - 1)/r_0}{1 + b_2 r_0} \right]^{-1}$$

freezing ($\propto 1/w$) initial growth ($\propto 1/n_{\mathrm{sat}}$)

Solution character

$\tau_f \gg \tau_g$: fast growth (high T, low w, small r_0) – the system loses memory about initial conditions

$\tau_f \ll \tau_g$: slow growth (low T, high w, large r_0) – vapor depletion controlled by frz haze distribution

Ice crystal number concentration as a function of vertical velocity, size and temperature

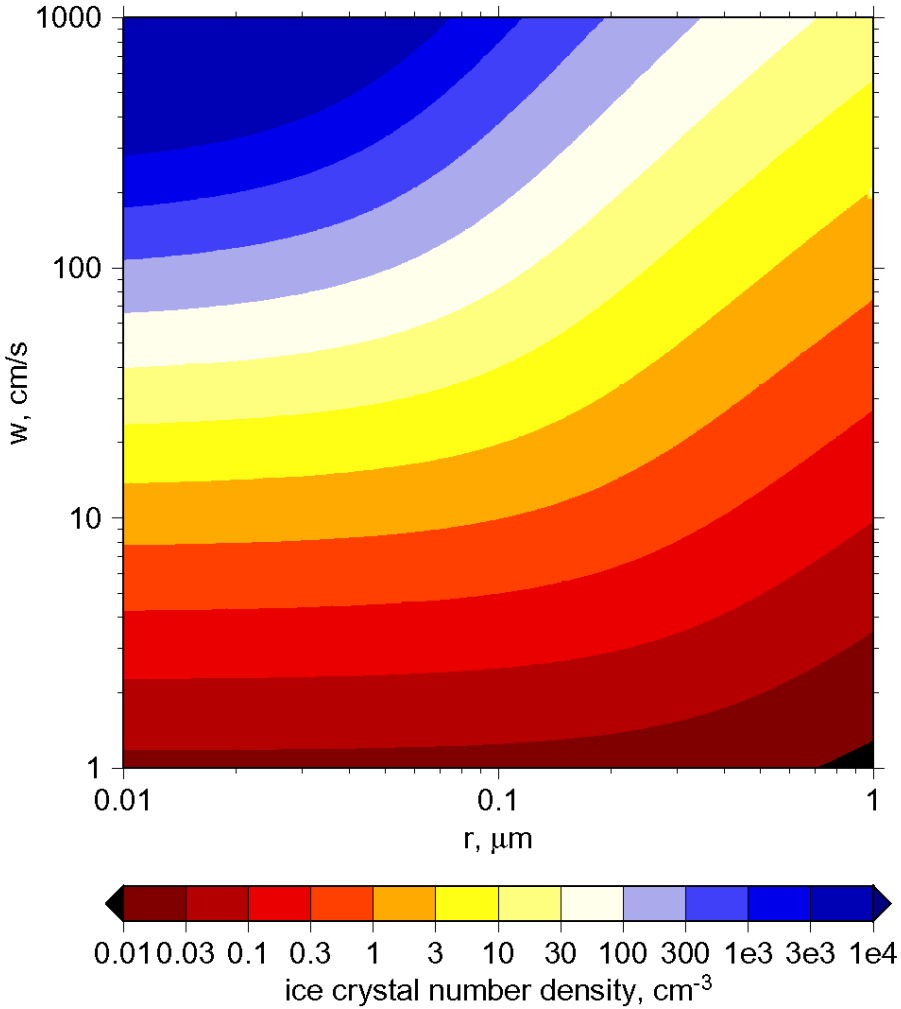

T=200 K

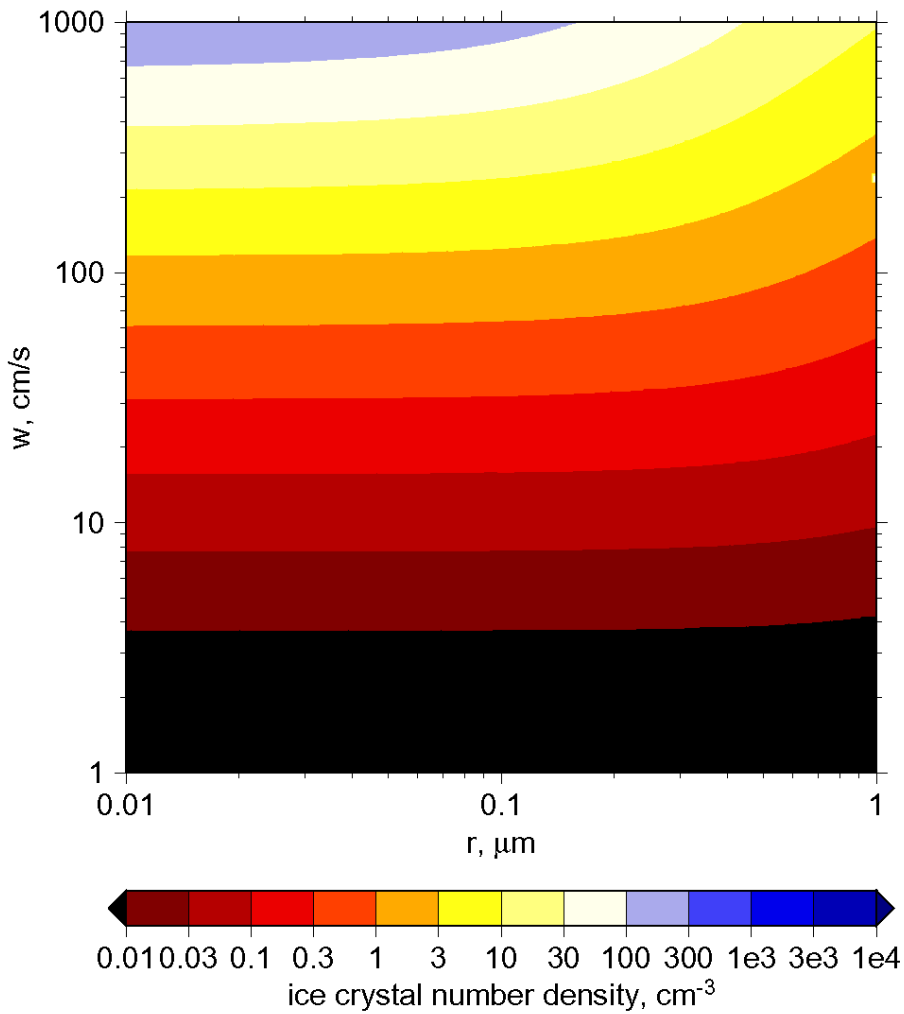

T=230 K

Homogeneous Freezing of Supercooled Aerosols

[Kärcher and Lohmann, 2002]

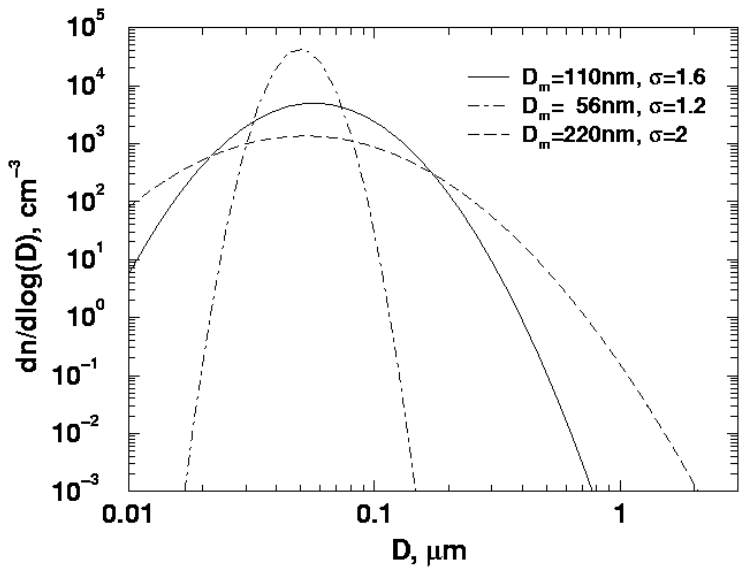

Parcel model results (symbols), parameterization (lines)

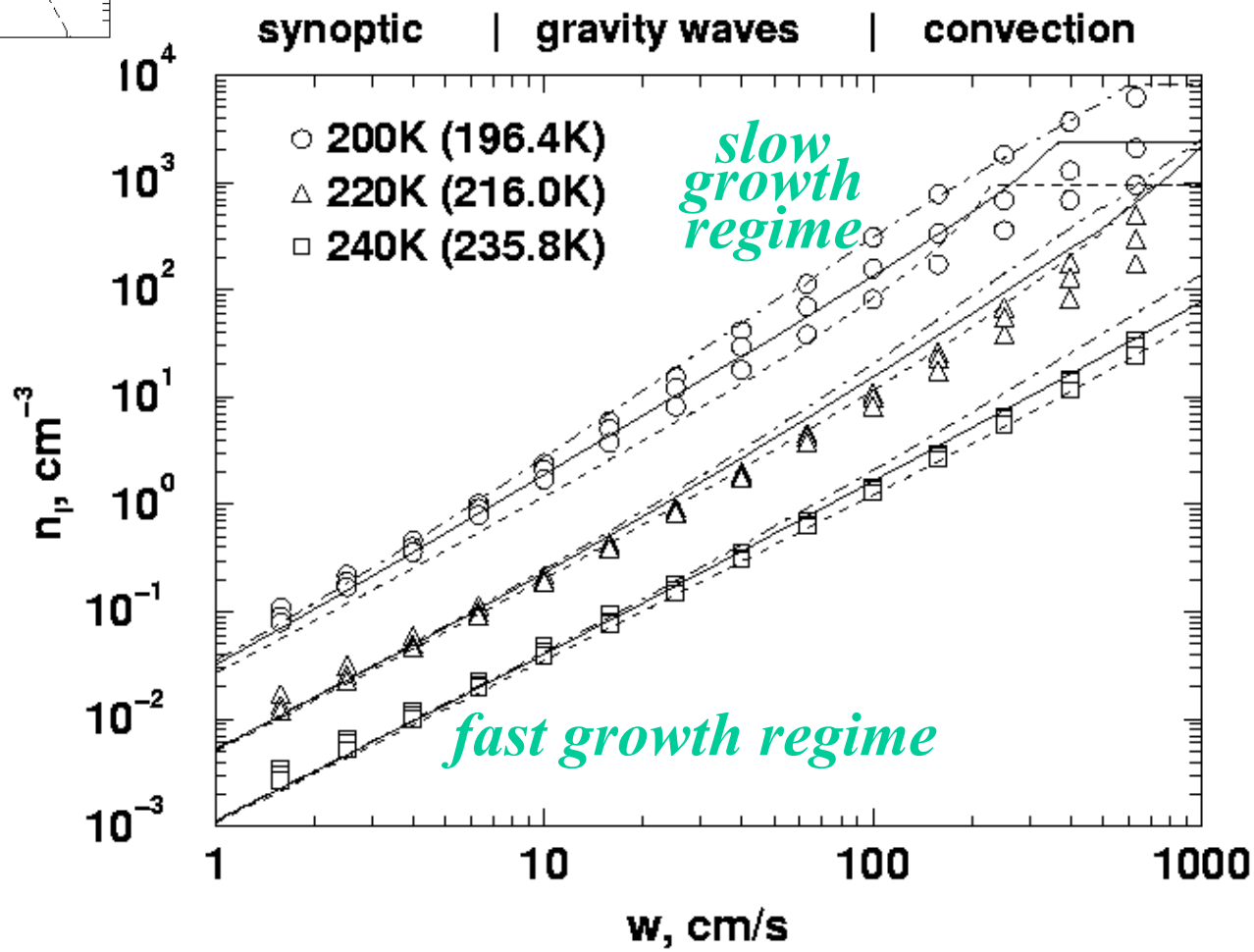

Homogeneous Freezing of Supercooled Aerosols

[Kärcher and Lohmann, 2002a,b; Lohmann and Kärcher, 2002]

- Obtain number of ice crystals n_i at critical supersaturation S_{cr}:

$$n_i = m_w/\rho_i \, [b_2/(2\pi \, b_1)]^{3/2} \, a_1 \, S_{cr}/(a_2 + a_3 \, S_{cr}) \, w \, \tau^{-1/2}$$

w = updraft velocity = sum of large-scale velocity and sub-grid scale enhancement (α TKE$^{1/2}$) in ECHAM4,

τ = freezing time scale, a_k,b_k = coefficients

- Note: No explicit dependence of nucleation rate on aerosol particle concentration n_a, but n_a serves as upper bound:

  n_a = sulfate + MSA + sea salt + dust + hydrophilic OC and BC

Updraft velocities and ice crystal number in NH

[Kärcher and Ström, 2003]

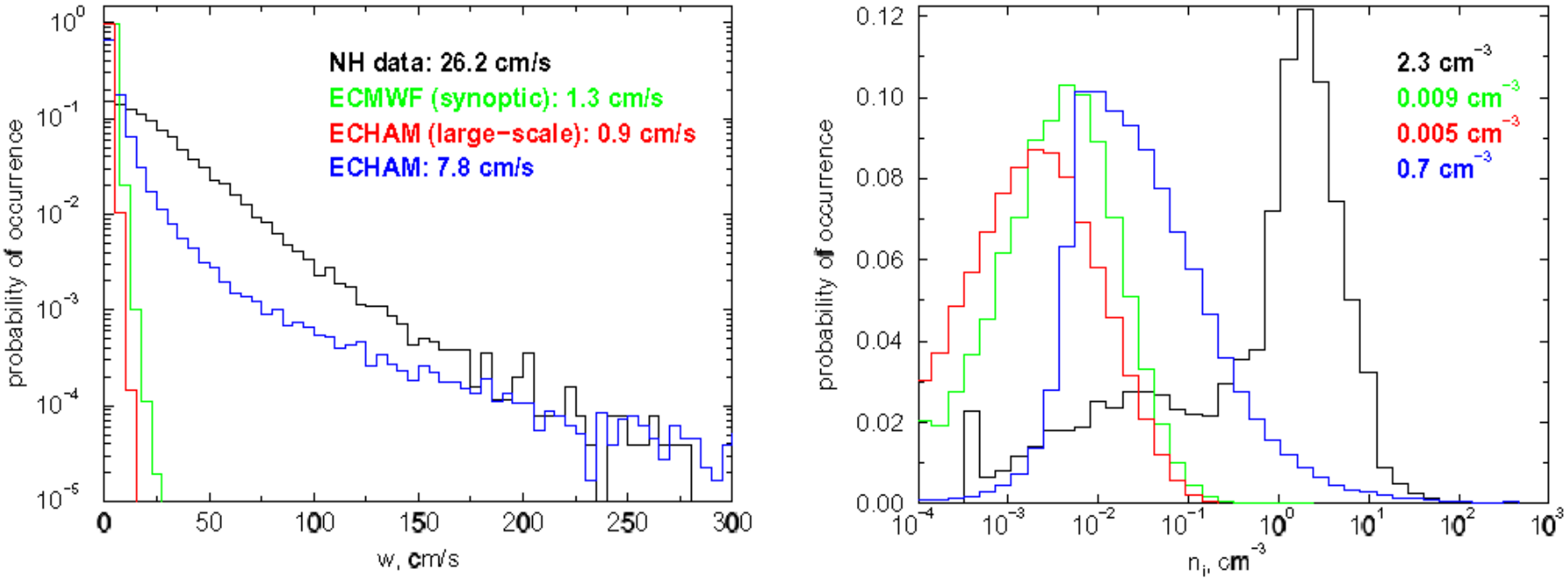

Fig. 8. Distributions of updraft speeds (left panel) from the NH data set (black), from upper tropospheric synoptic-scale winds caluclated by the ECMWF weather forecast model (green), from upper tropospheric large-scale winds caluclated by the ECHAM general circulation model (red), and from corresponding ECHAM simulations where subgrid-scale fluctuations are added to the large-scale vertical wind to approximately account for mesoscale variability (blue). The distributions of n_i obtained from calculations are shown in the right panel. No additional artificial noise or wave-driven variability was added to calculate the distributions of n_i.

Relative Humidity over the North Atlantic

Mozaic observations: Gierens et al.[1999]

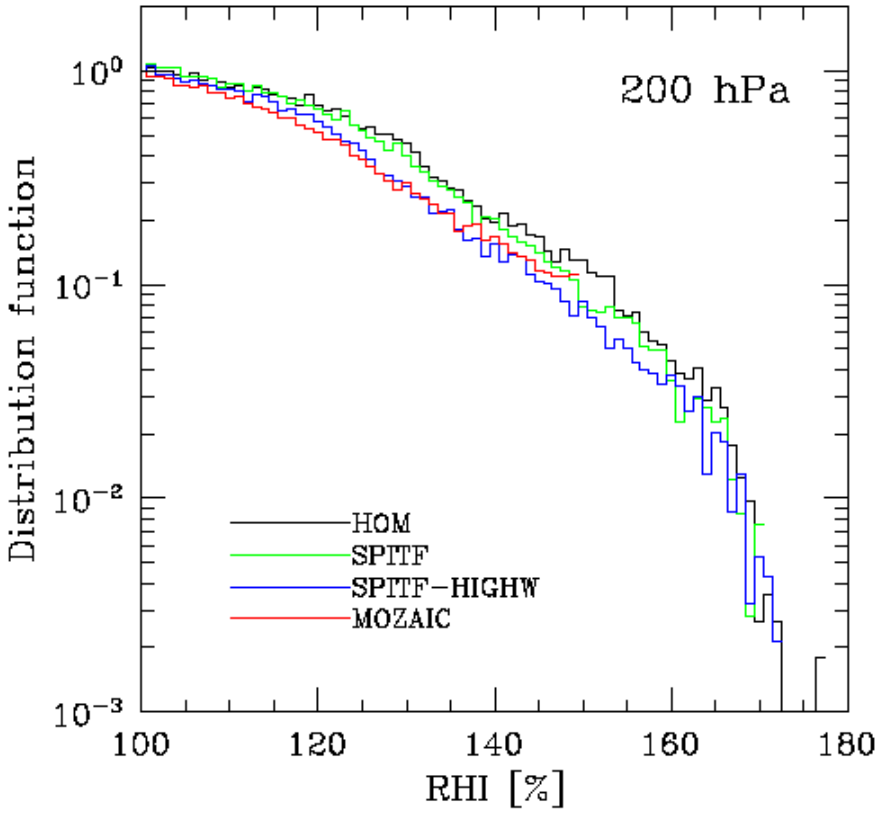

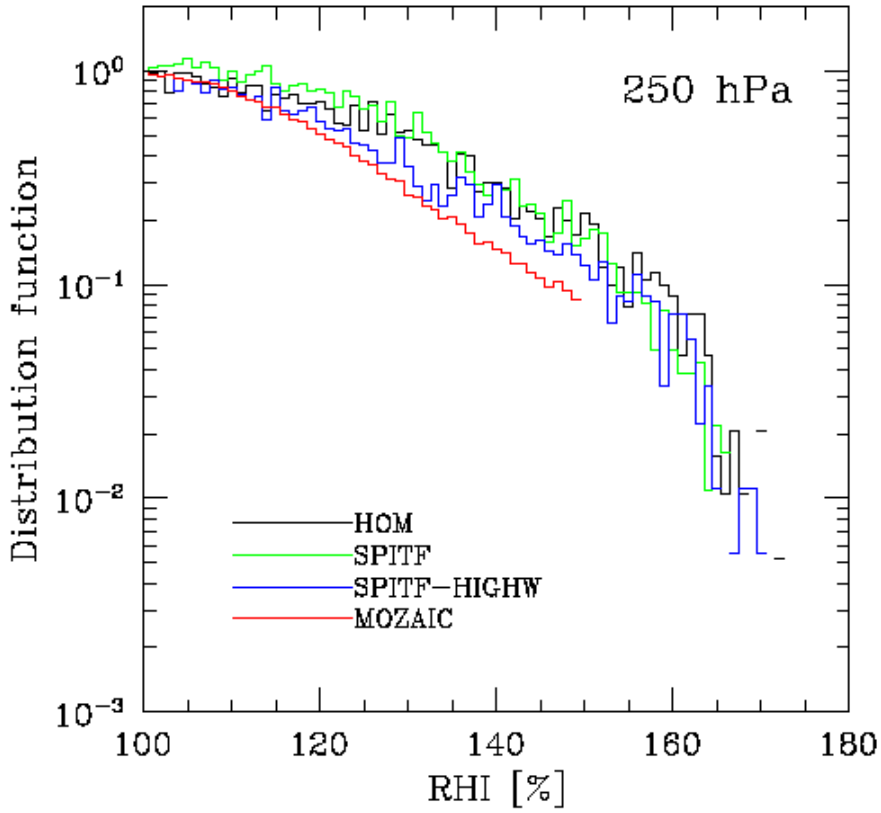

[Haag et al. 2003]

Pinatubo studies with ECHAM4

[Lohmann, Kärcher, Timmreck, 2003]

- T30 horizonal resolution (3.75° x 3.75°) with 19 vertical levels and top at 10 hPa
- Use climatological sea surface temperature to isolate the effect of the volcanic eruption
- Sensitivity experiments (July 1991 – December 1993):
  - *HOM:* Homogeneous freezing of monomodal aerosol particles
  - *HOM-Size:* Assume bimodal aerosol size distribution (accumulation and coarse mode)
  - *HOM-Pin:* Add sulfate aerosol mass from Pinatubo: 17 Mt SO_2 between 0°-19°N, 96°E -118°E, 21.5-29 km *[Timmreck et al. 1999]* assuming a monomodal aerosol size distribution $\Rightarrow$ more representative for shortly after the eruption
  - *HOM-Pin-Size:* Assume trimodal aerosol size distribution (add Pinatubo aerosol) $\Rightarrow$ more representative for 1992

Trimodal Aerosol Size Distribution

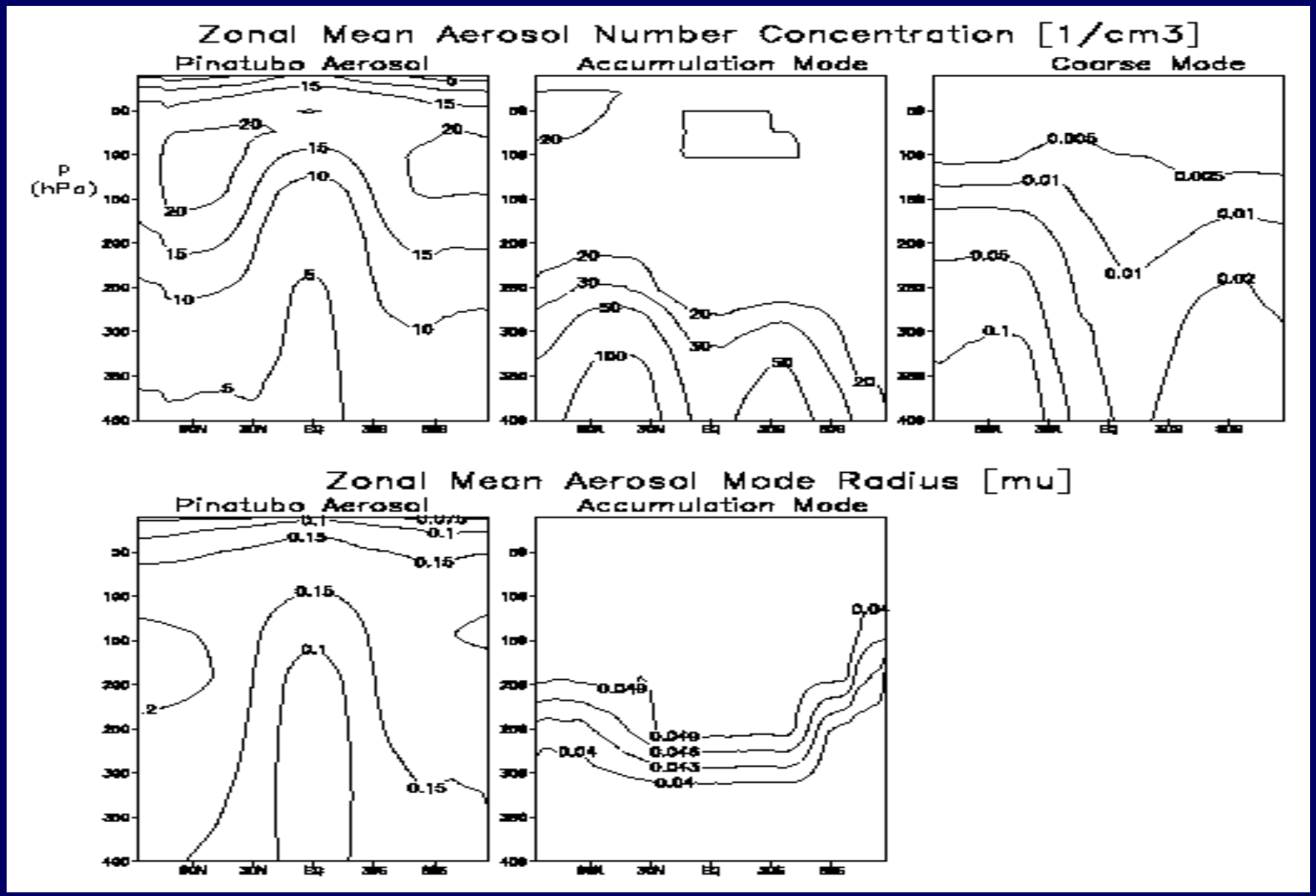

Temporal Evolution (July 1991-Dec 1993) of Aerosol and Ice Crystal Number Concentrations

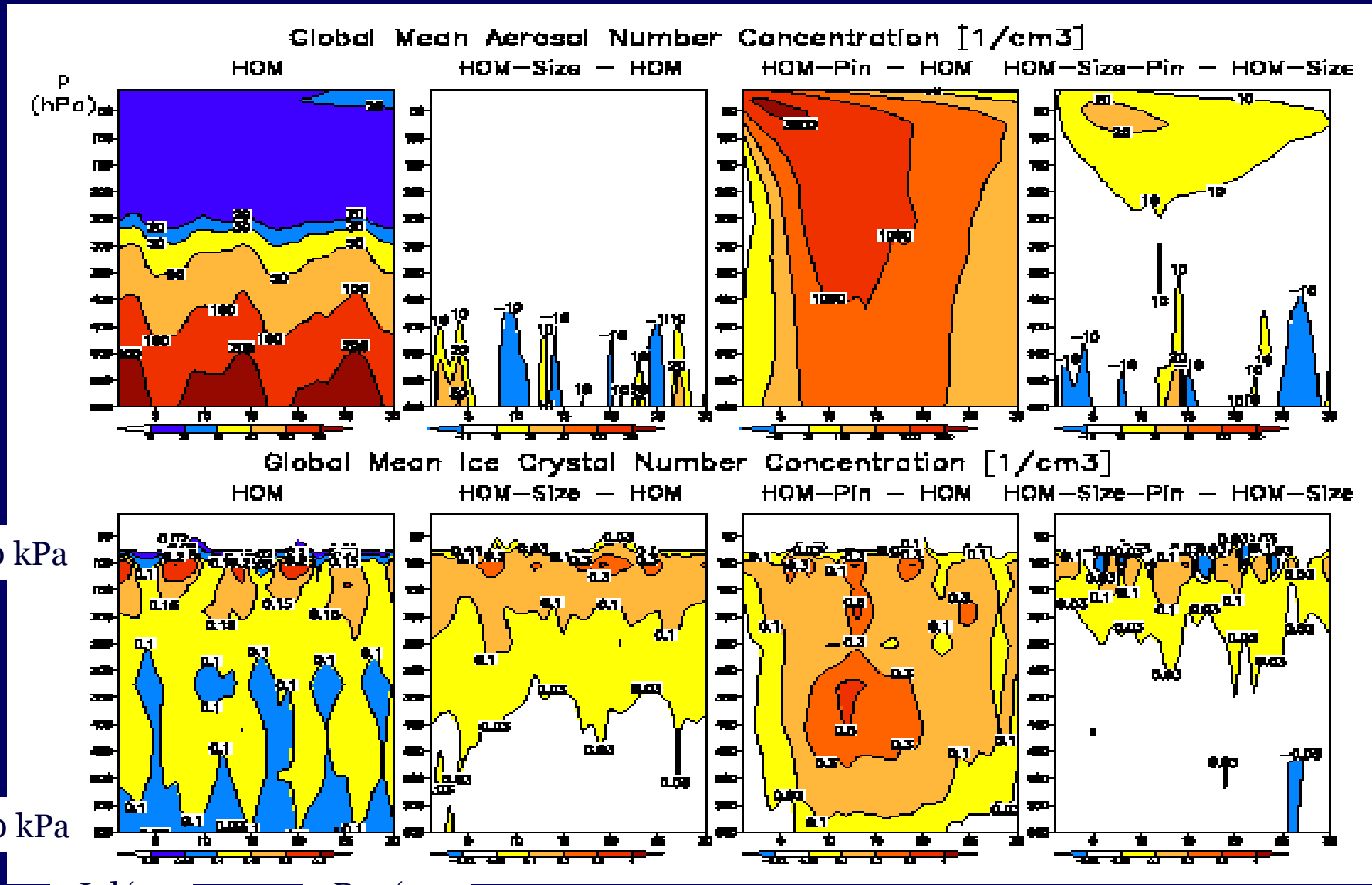

Temporal Evolution of Cloud Properties in the Tropics after the Mt. Pinatubo Eruption

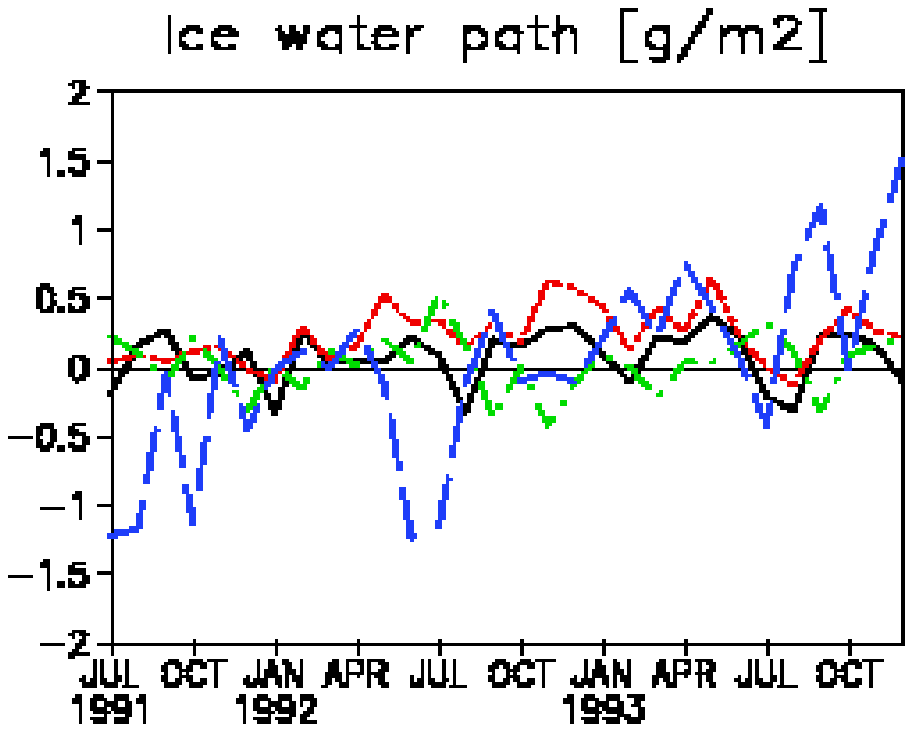

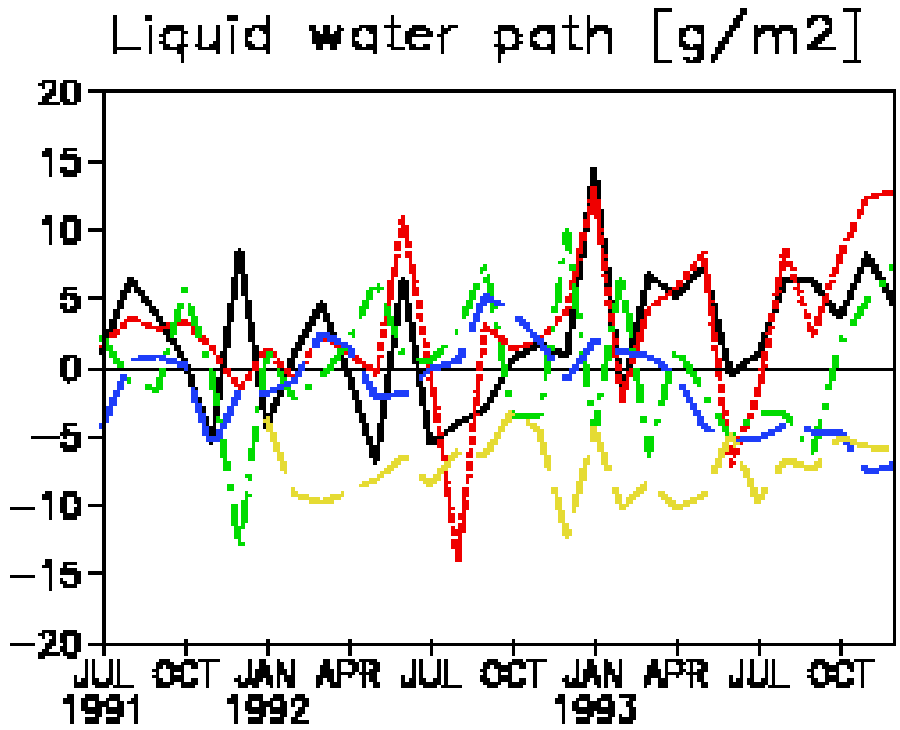

LEGEND: *HOM-Size –HOM ; HOM-Pin –HOM (representative for shortly after eruption); HOM-Pin-Size –HOM-Size (representative for 1992)*

ISCCP Satellite Observations, SSM/I Observations

[Lohmann, Kärcher, Timmreck, 2003]

Conclusions homogeneous freezing:

- ECHAM4 captures the observed distribution law of supersaturation with respect to ice in cloud-free regions.
- Subgrid-scale enhancement of vertical velocity is crucial to obtain ice crystal number concentrations of the same order of magnitude as observed.
- The simulated increase in aerosol and ice crystal number concentrations after the Mt. Pinatubo eruption depends crucially on the assumed aerosol size distribution.
- Effects from the Mt. Pinatubo eruption on clouds and climate considering only homogeneous freezing are small.

Which aerosols act as ice nuclei?

Liquid ammonium sulfate particles with solid kaolinite inclusions:

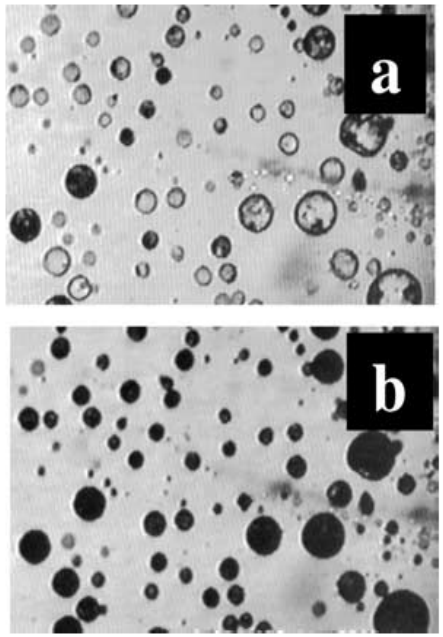

Figure 1. (a) Liquid ammonium sulfate particles with solid kaolinite inclusions. (b) Same particles with kaolinite inclusions, after freezing.

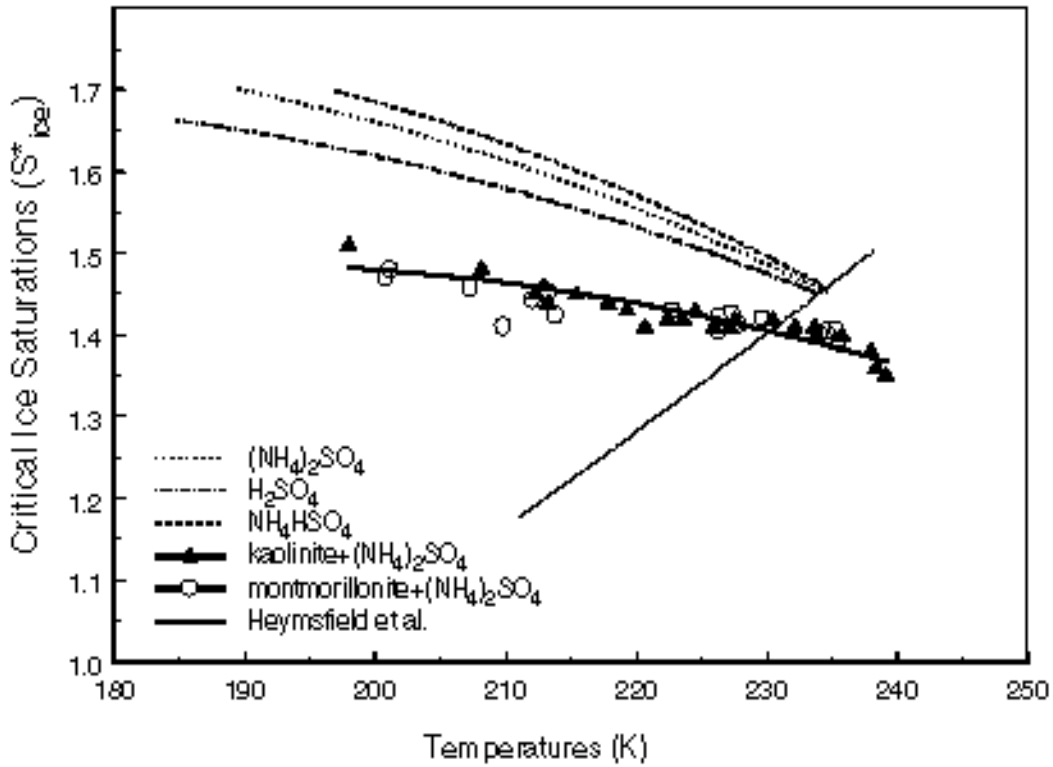

[Zuberi et al., 2002]

Which aerosols act as ice nuclei?

Soot:

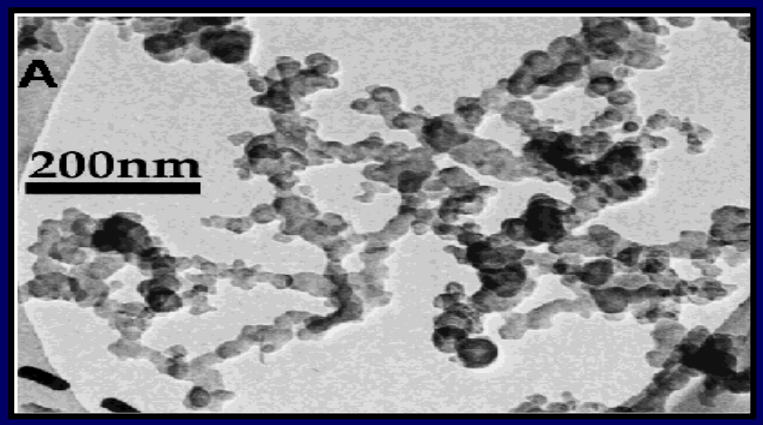

Soot covered by sulfuric acid:

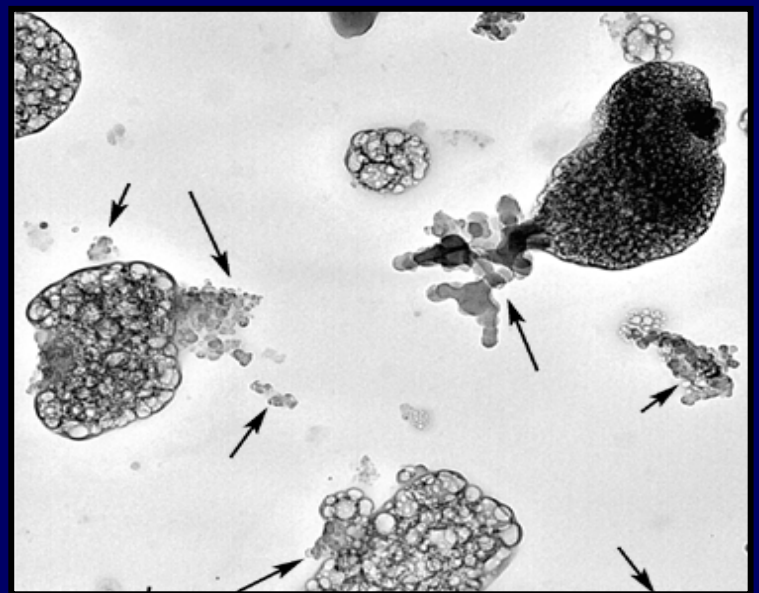

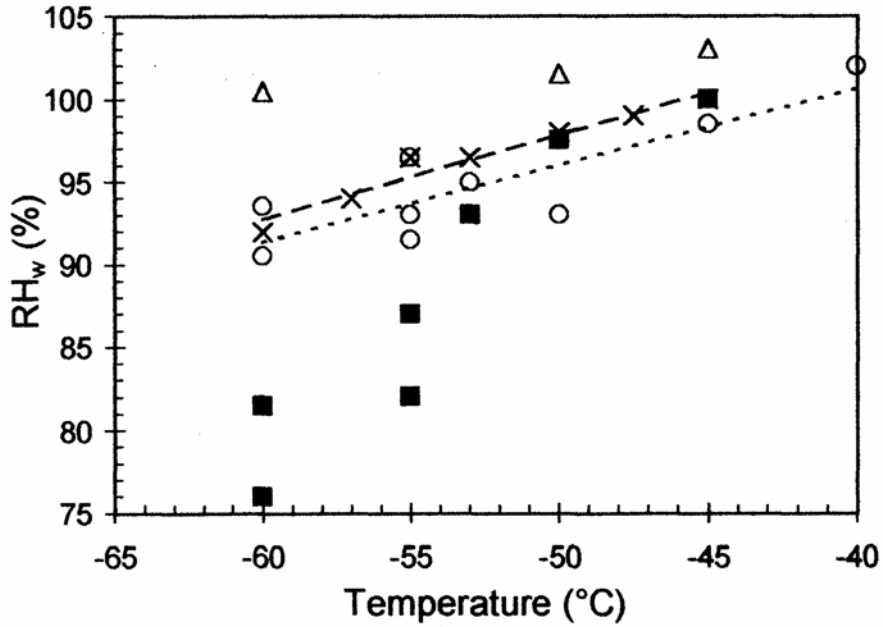

Figure 4. Summary of conditions for ice formation by 1% of soot particles subjected to different treatments. Linear regression fits to the data from experiments with untreated soot (o) and soot treated with an approximate monolayer of H_2SO_4 (×) are indicated, respectively, by the short-dashed ($r^2 = 0.95$) and long-dashed ($r^2 = 0.73$) lines. Experiments with multi-layer H_2SO_4 coverage are indicated by the filled square symbols. Experimental conditions for ice formation on small (<20 nm) pure sulfuric acid particles are given by triangle symbols.

[DeMott et al., 1999]

Heterogeneous Freezing of Supercooled Aerosols

[Water activity a_w ~ relative humidity]

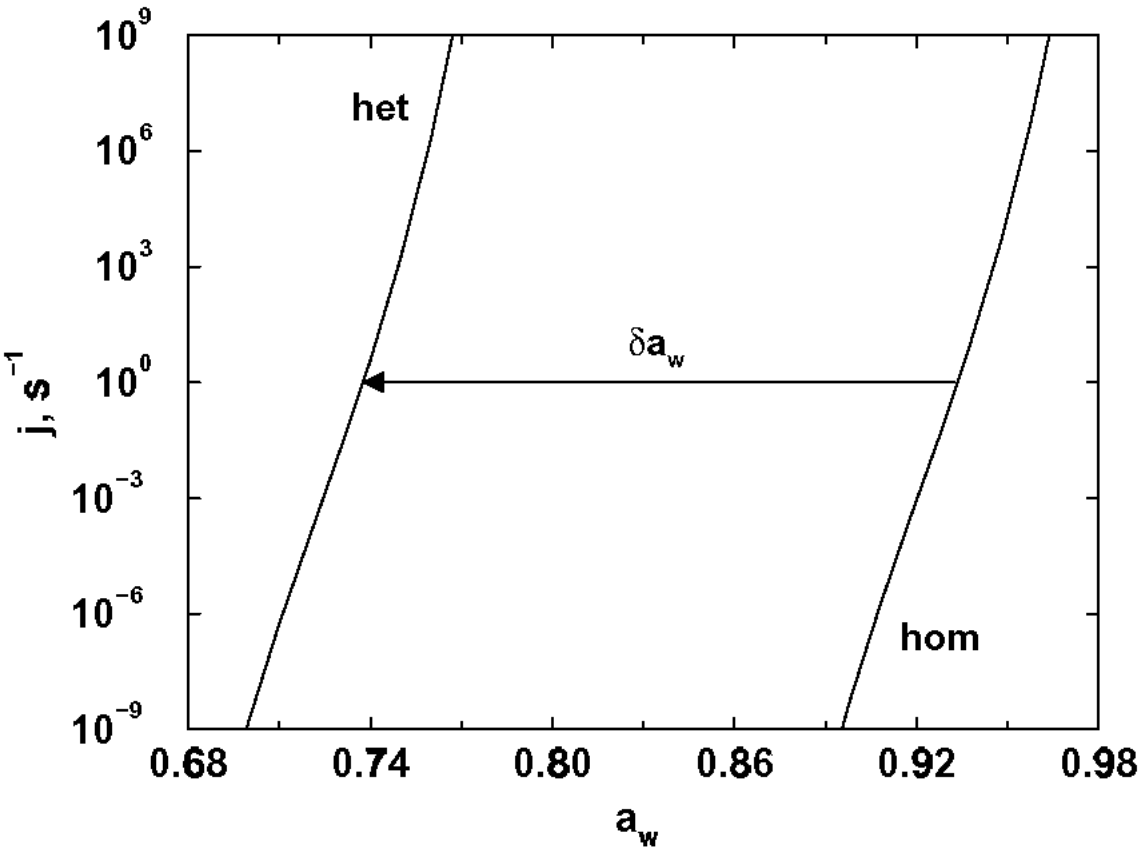

Figure 2. Nucleation rates per particle per second versus water activity at 220 K. Homogeneous (right curve) and heterogeneous (left curve) are shifted by the amount $\delta a_w \simeq 0.2$ resulting from $S_{cr}^{het} = 1.2$. The same particle that freezes homogeneously at $a_w \simeq 0.93$ would freeze heterogeneously at $a_w \simeq 0.73$ under these conditions.

Heterogeneous Freezing of Supercooled Aerosols

[Kärcher and Lohmann, 2003]

Assume that heterogeneous freezing can be represented by a reduction in super-saturation required for freezing

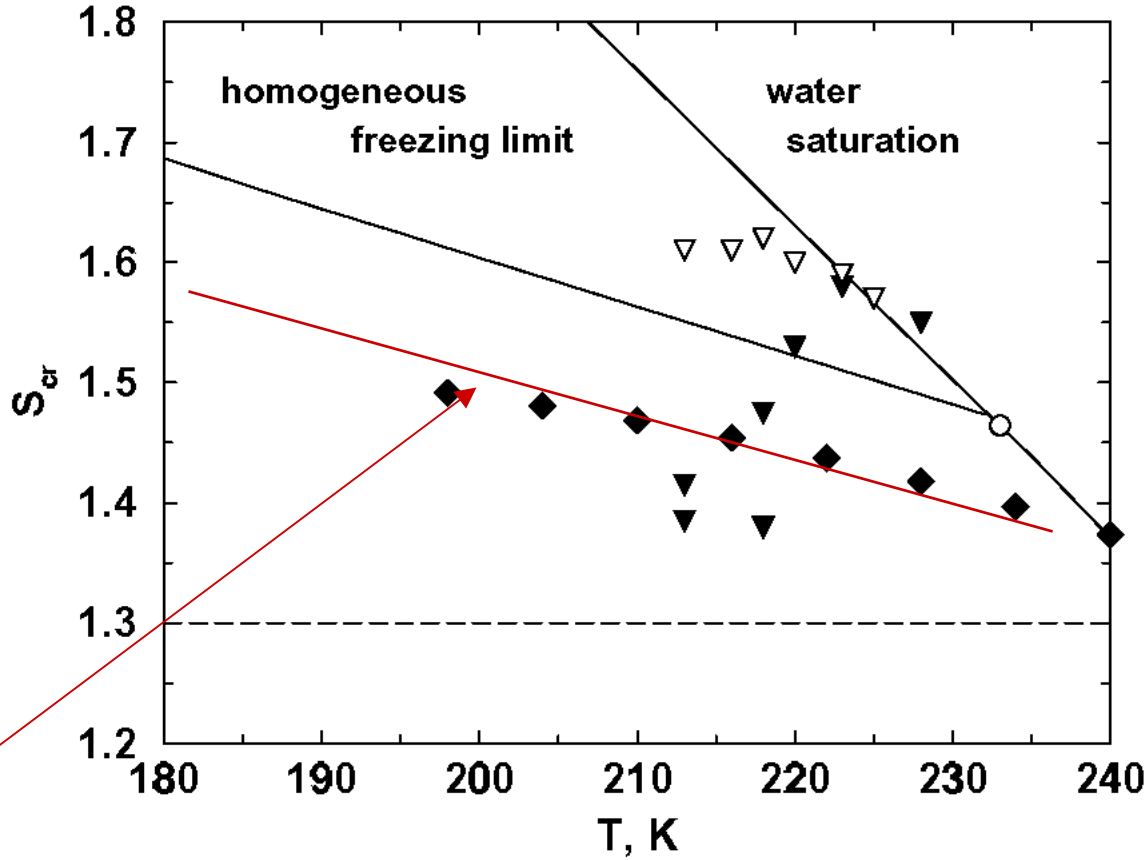

Figure 3. Freezing threshold saturation ratios over ice versus temperature for homogeneous freezing (upper left solid curve) from (5) and for a constant value of 1.3 (dashed line). The upper right solid curve shows the ice saturation ratios where liquid water would be saturated. Homogeneous freezing at temperatures to the right of the open circle occurs at water saturation. Also shown are experimental data for black carbon (BC) particles from DeMott et al. [1999] (filled/open triangles for multilayer/monolayer coverage with H_2SO_4) and for ammonium sulfate particles with mineral dust immersions from Zuberi et al. [2002] (diamonds). The latter authors have fitted their data to a shifted water activity.

Ice particle concentration for heterogeneous versus homogeneous freezing of supercooled aerosols

[Kärcher and Lohmann, 2003]

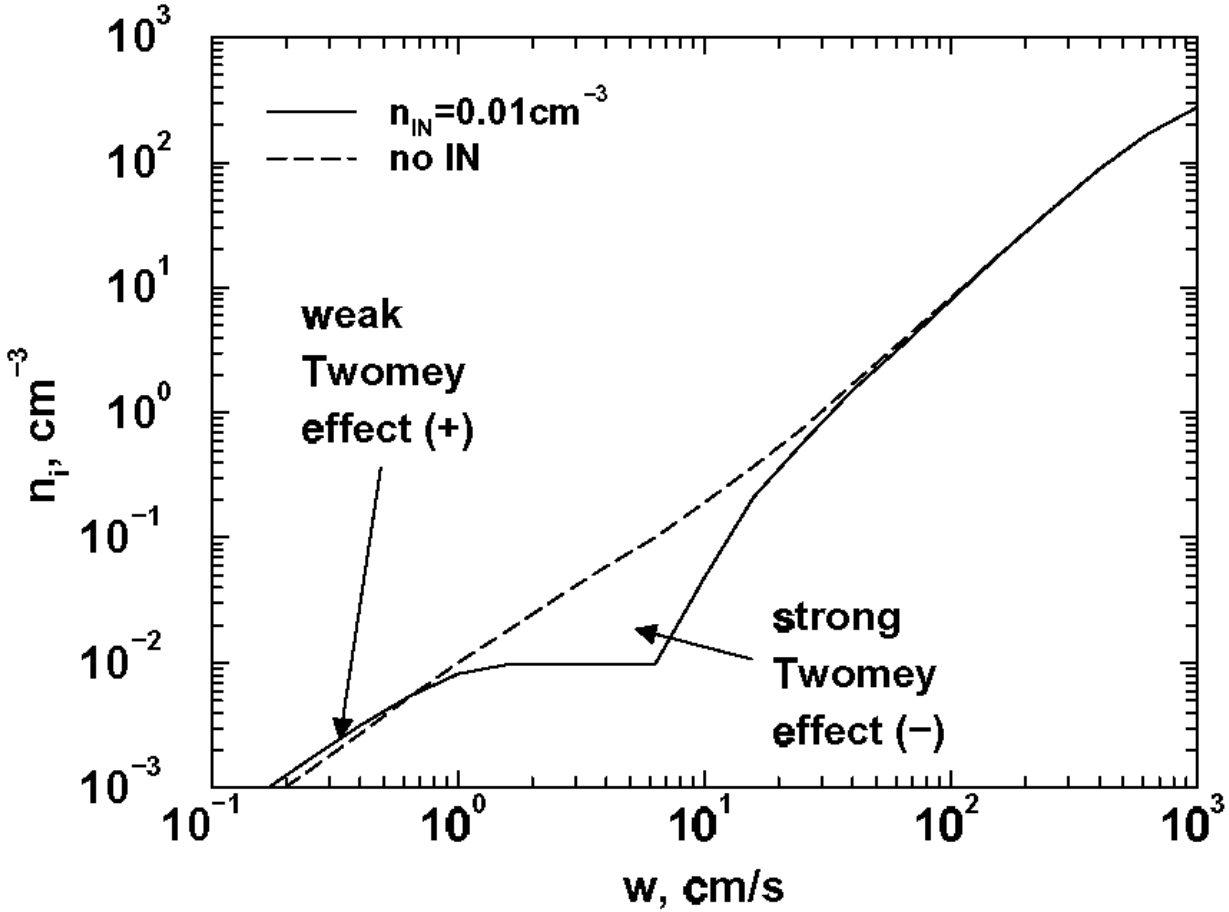

Figure 9. Number density of ice particles versus vertical velocity from APSC simulations starting at 225 K and ice saturation. In the model, 400 cm^{-3} homogeneous nuclei are present with 0.01 cm^{-3} (solid curve) and without (dashed curve) heterogeneous IN with $S_{cr}^{het} = 1.3$.

Annual, zonal mean latitude versus pressure heterogeneous (HET-IN) & homogeneous freezing (HOM)

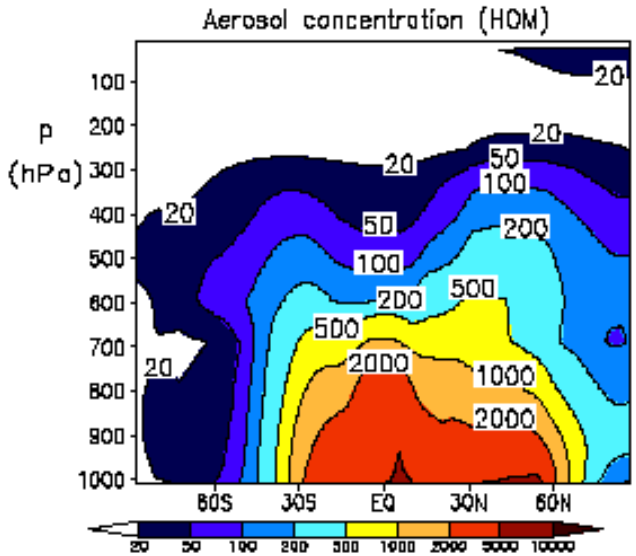

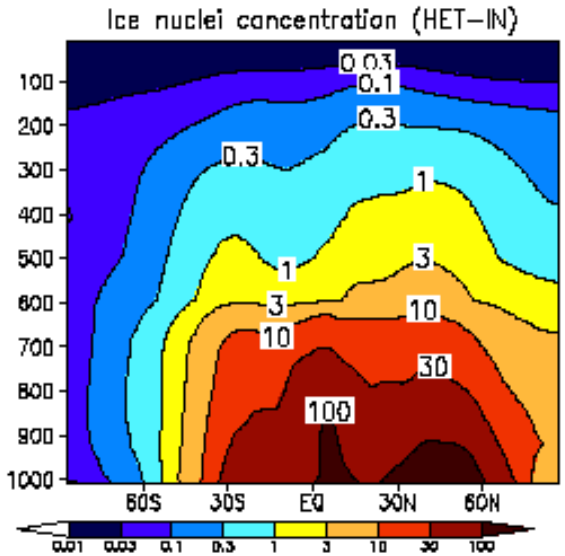

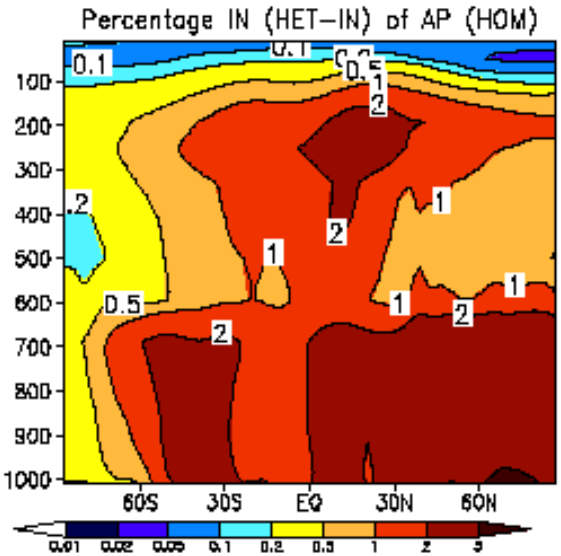

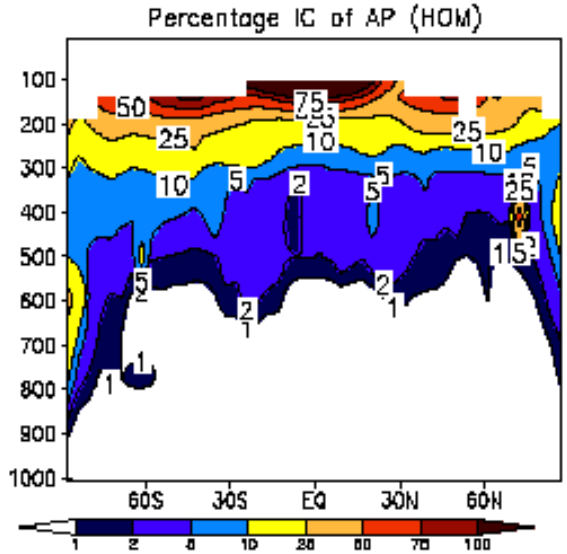

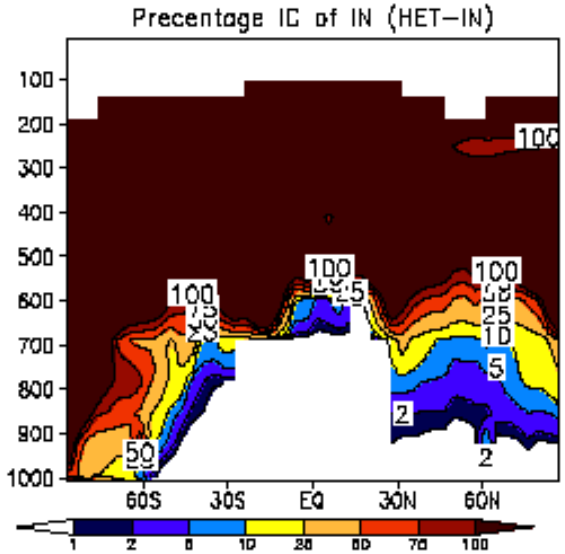

HET-IN: black carbon and dust act as immersion nuclei

Aerosol conc. [cm^{-3}]
Ice nuclei conc. [cm^{-3}]

Vertically integrated annual mean cirrus crystal number formed by homogeneous and heterogeneous freezing

HOM (crystals cm^{-2} s^{-1}) HET–IN

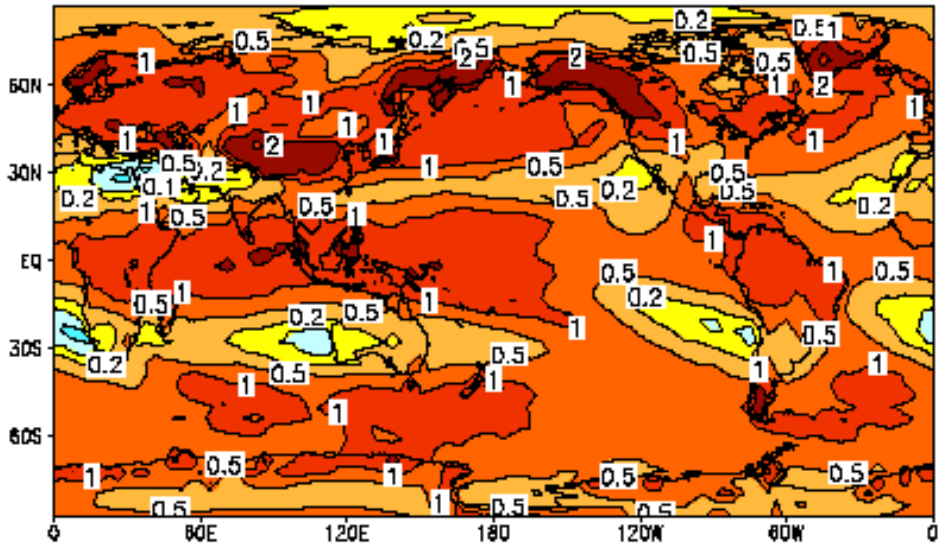

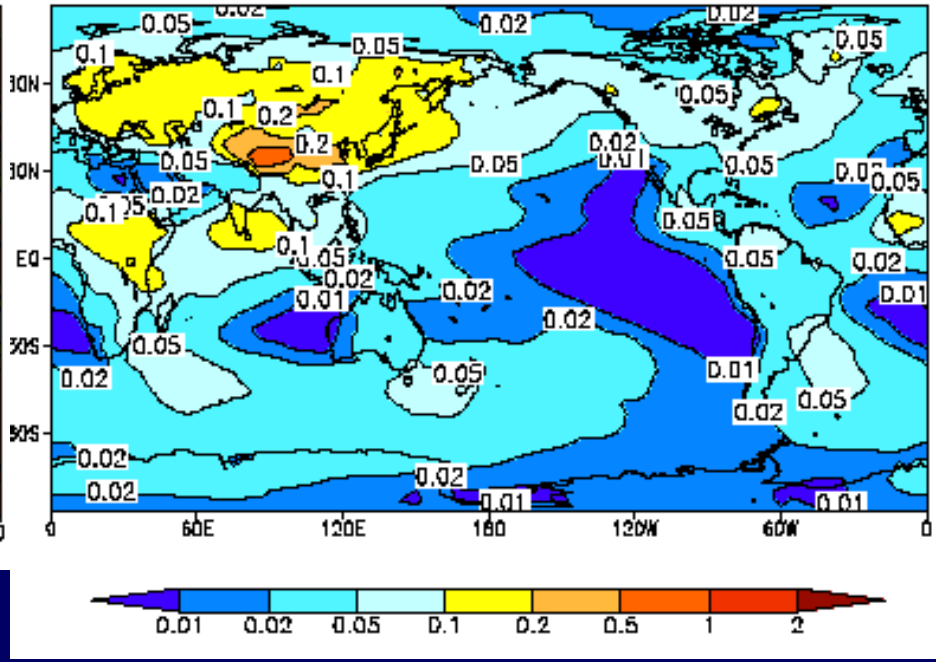

Annual, zonal mean latitude versus pressure ice crystal concentration (cm^{-3})

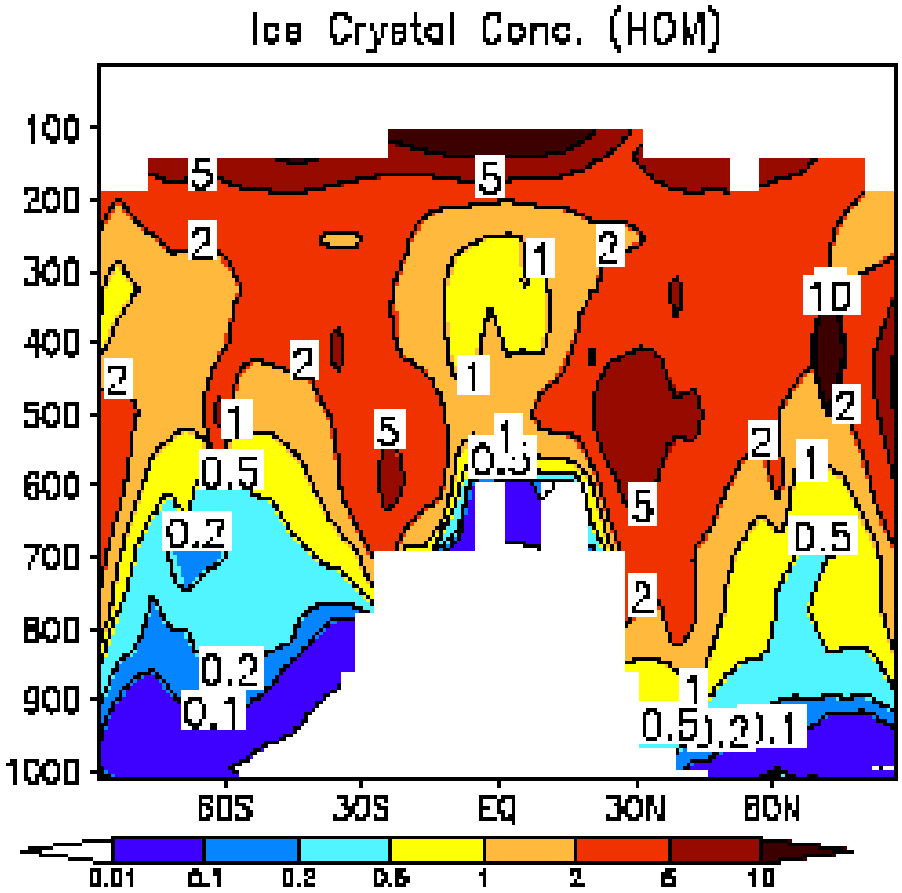

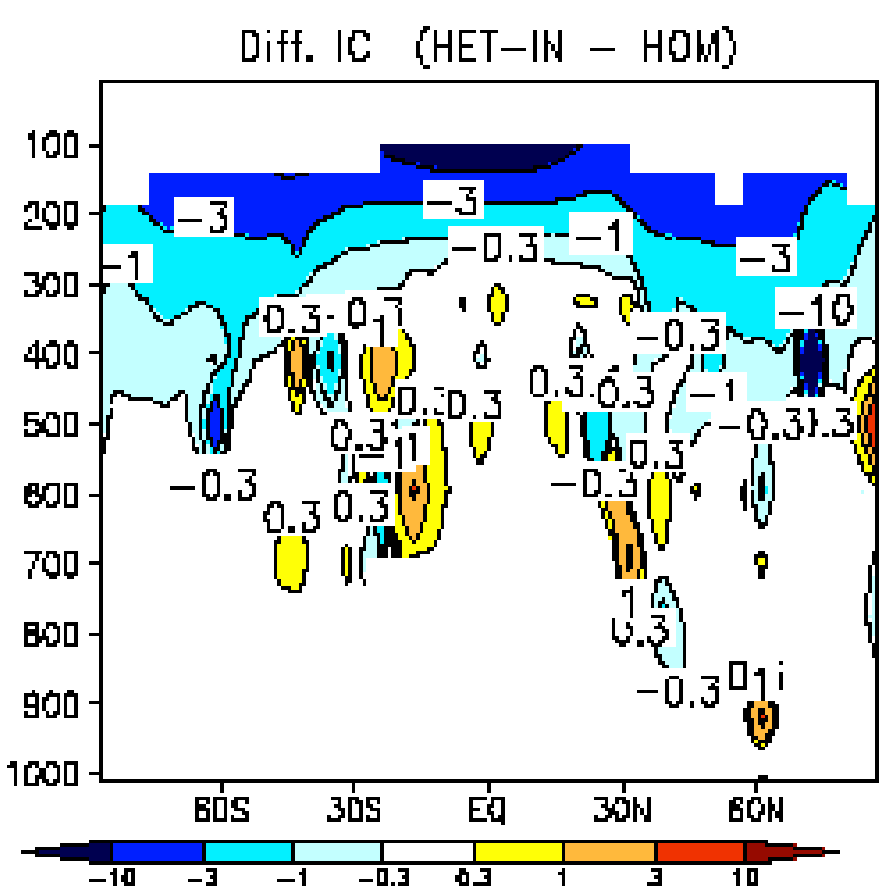

Global annual mean simulations of heterogeneous (HET) versus homogeneous (HOM) freezing

Legend:
HOM,
HET-IN,
HET-100%
Observations

Ice water path [g/m²]
Ice crystal number [10^6 cm^{-2}]
Precipitation [mm/d]
Total cloud cover [%]

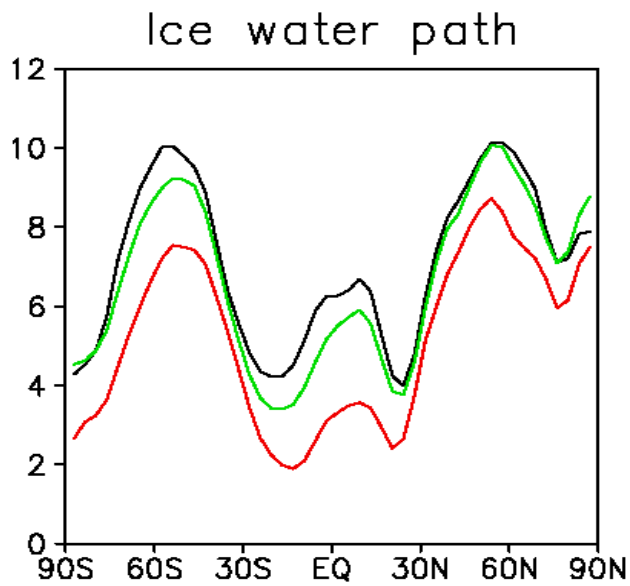

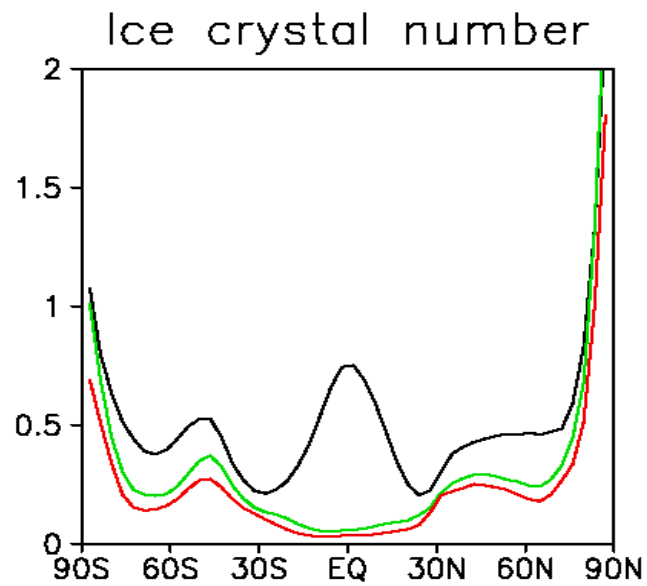

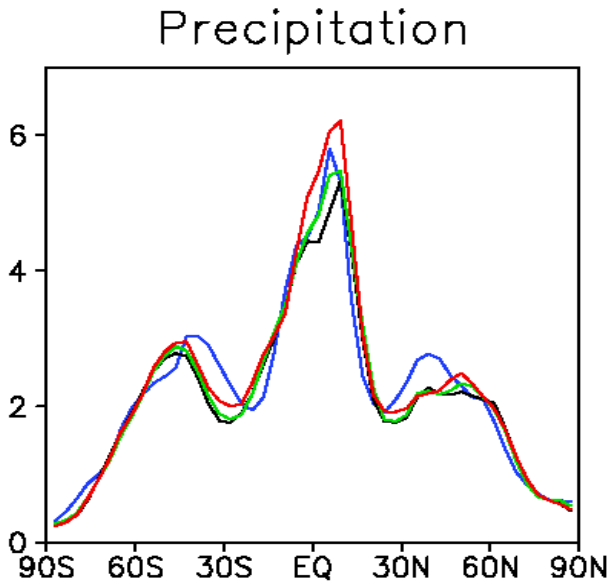

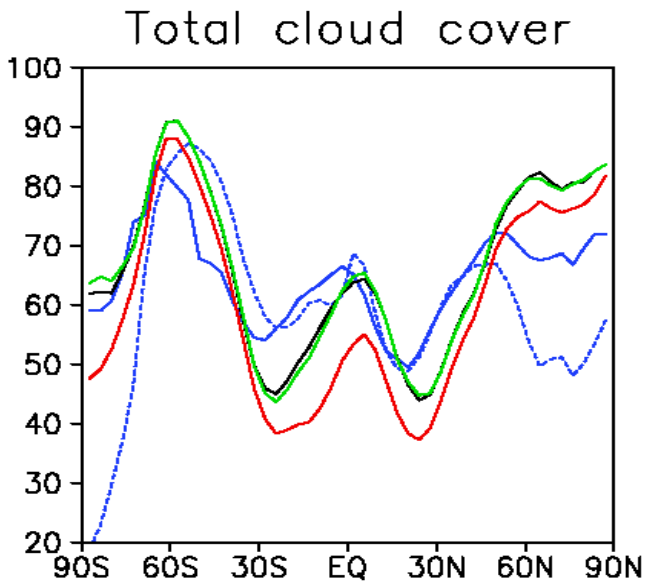

Normalized frequency distribution of relative humidity with respect to ice (RHi)

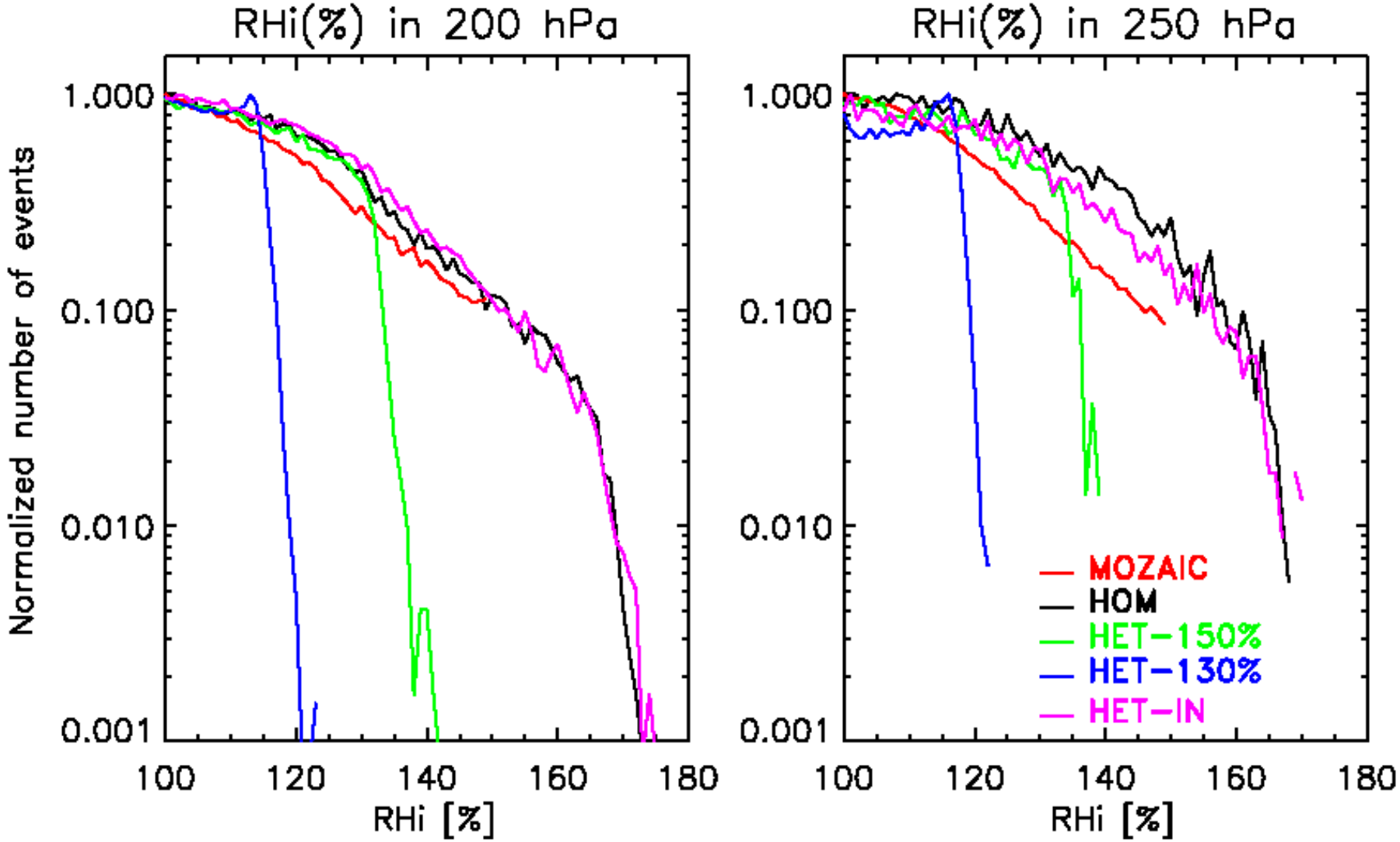

Global annual mean quantities in the homogeneous (HOM) and heterogeneous freezing (HET) simulations

	HOM	HET-IN	HET-100%
Ice water path [g m^{-2}]	6.8	6.2	4.8
SW radiation TOA [W m^{-2}]	238	240	242
LW radiation TOA [W m^{-2}]	231	234	239
Total cloud cover [%]	62.3	62.1	55.4
Total precipitation [mm/d]	2.62	2.69	2.83

Conclusions heterogeneous freezing:

- Parcel model results show that a positive or negative first indirect aerosol effect (Twomey effect) on cirrus clouds is possible depending on the vertical velocity and on the properties of the ice nuclei.

- Climate model results of different heterogeneous freezing simulations show that heterogeneous freezing leads to fewer ice crystals than formed by homogeneous freezing. These fewer ice crystals grow to larger size, thus increasing global mean precipitation and decreasing total cloud cover.

ECHAM4 Accumulation Mode Aerosol Validation

Johannes Hendricks, personal communication [2003]

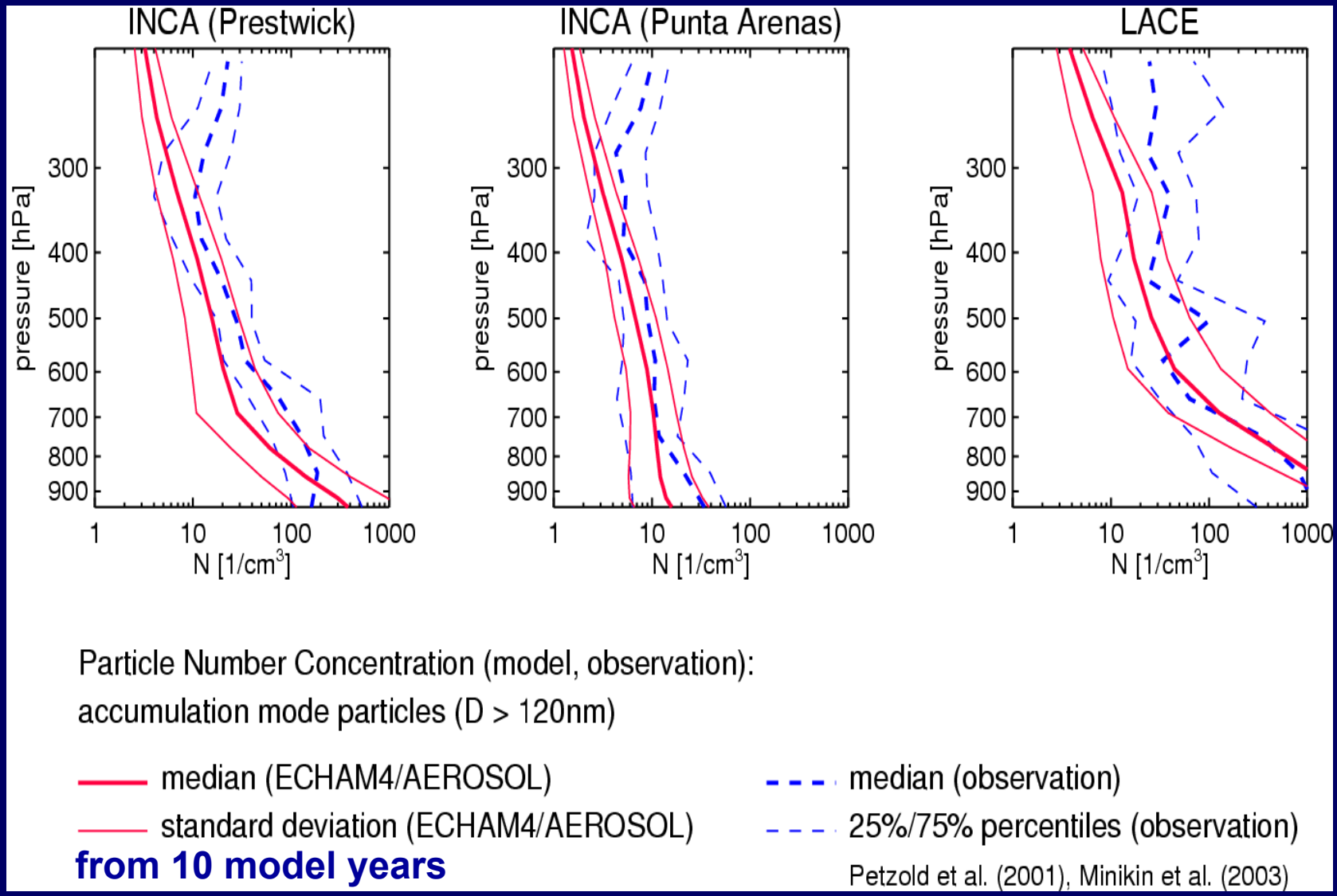

Particle Number Concentration (model, observation):

accumulation mode particles (D > 120nm)

median (ECHAM4/AEROSOL)

standard deviation (ECHAM4/AEROSOL)

median (observation)

25%/75% percentiles (observation)

from 10 model years

Petzold et al. (2001), Minikin et al. (2003)

Vertical velocity (w) in Chile (54°S) and Scotland (53°N)

[Aircraft data from INCA campaign: Ström et al. 2002]

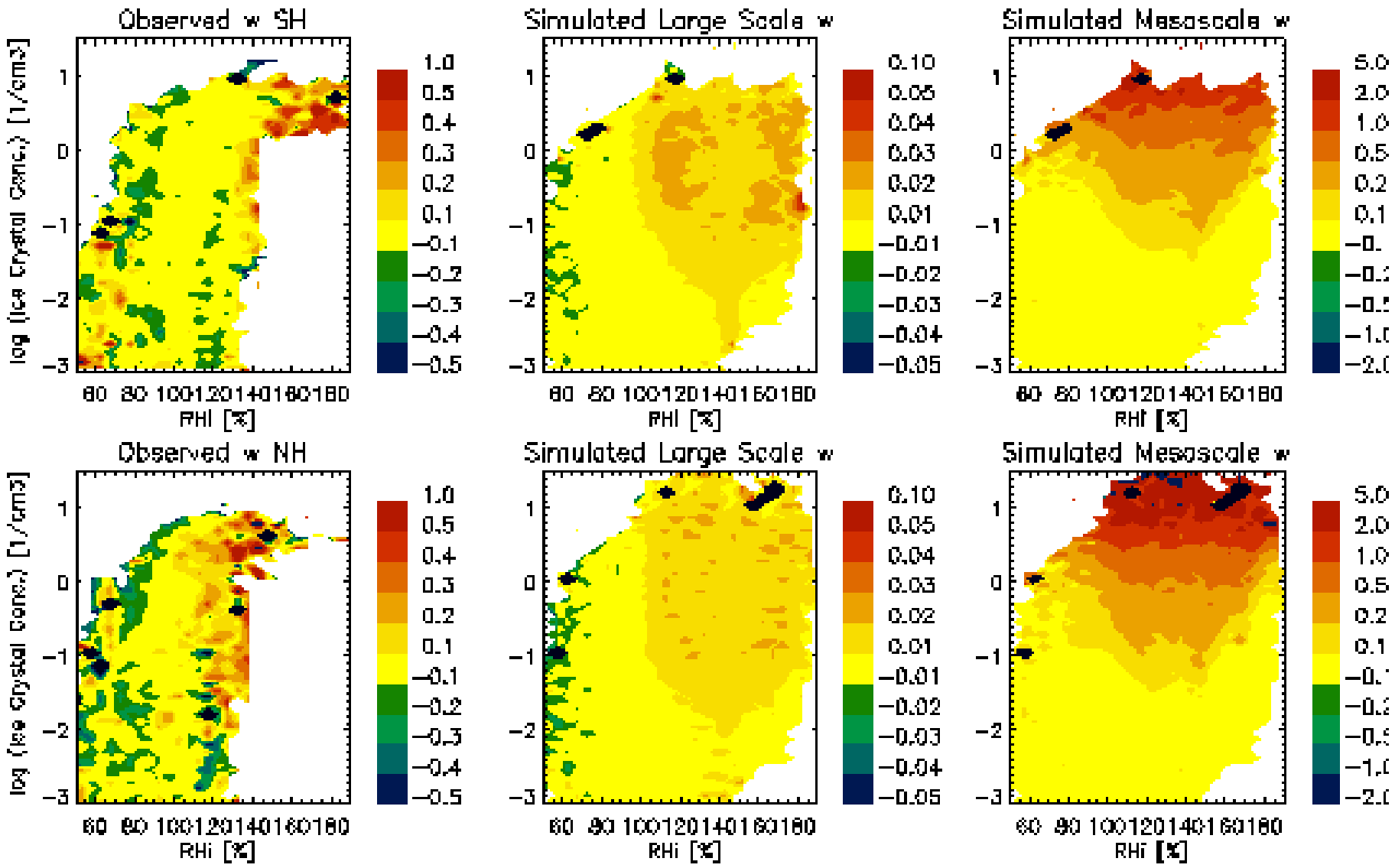

Temporal Evolution of Cloud Radiative Forcing [W/m²] after the Mt. Pinatubo Eruption

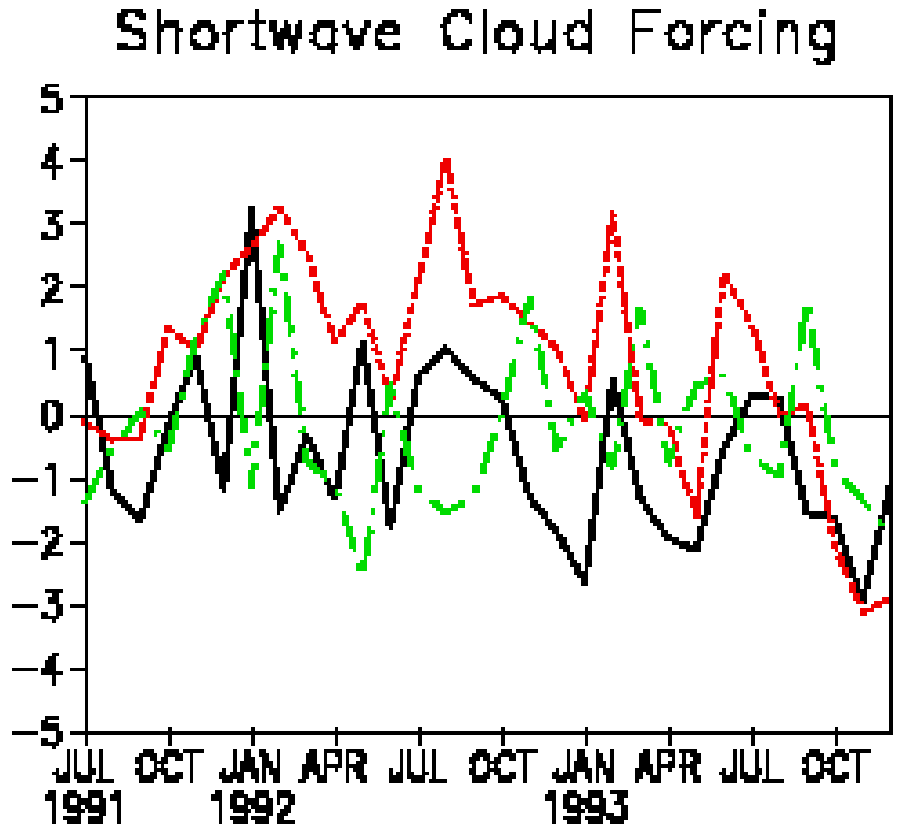

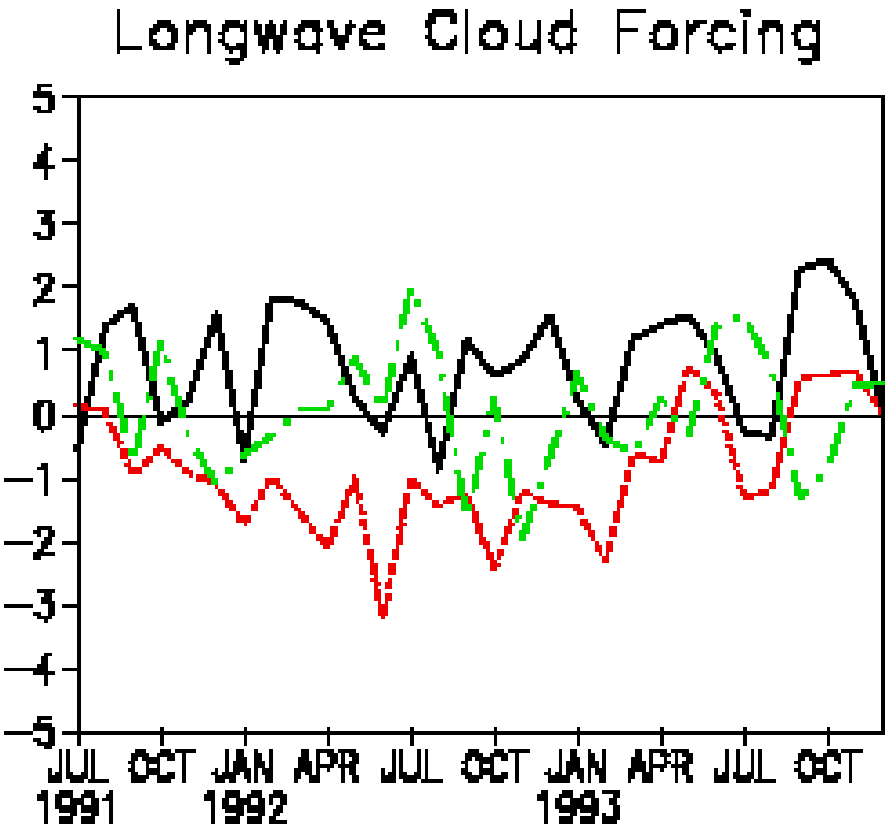

LEGEND: ***HOM-Size –HOM ; HOM-Pin –HOM (representative for shortly after eruption); HOM-Pin-Size –HOM-Size (representative for 1992)***

[Lohmann, Kärcher, Timmreck, 2003]